

In Situ NMR Observation of Mono- and Binuclear Rhodium Dihydride Complexes Using Parahydrogen-Induced Polarization

Andreas Koch and Joachim Bargon*

Institute of Physical and Theoretical Chemistry, University of Bonn,
Wegelerstrasse 12, D-53115 Bonn, Germany

Received November 12, 1999

Starting from the binuclear complex $[\text{RhCl}(\text{NBD})_2]$ (NBD = 2,5-norbornadiene) in the presence of the phosphines $\text{L} = \text{PMe}_3, \text{PMe}_2\text{Ph}, \text{PMePh}_2, \text{PEt}_3, \text{PEt}_2\text{Ph}, \text{PEtPh}_2,$ or $\text{P}(n\text{-butyl})_3$, various mononuclear dihydrides of the type $\text{Rh}(\text{H})_2\text{CIL}_3$, i.e., those of the homogeneous hydrogenation catalysts RhCIL_3 , have been obtained upon addition of parahydrogen, and their ^1H NMR spectra have been investigated using parahydrogen-induced polarization (PHIP). Furthermore, the two binuclear complexes $(\text{H})(\text{Cl})\text{Rh}(\text{PMe}_3)_2(\mu\text{-Cl})(\mu\text{-H})\text{Rh}(\text{PMe}_3)$ and $(\text{H})(\text{Cl})\text{Rh}(\text{PMe}_2\text{Ph})_2(\mu\text{-Cl})(\mu\text{-H})\text{Rh}(\text{PMe}_2\text{Ph})$ have been detected and characterized by means of this in situ NMR method. Analogous complexes with trifluoroacetate instead of chloride, i.e., $\text{Rh}(\text{H})_2(\text{CF}_3\text{COO})\text{L}_3$, have been generated in situ starting from $\text{Rh}(\text{NBD})(\text{acac})$ in the presence of trifluoroacetic acid in combination with the phosphines $\text{L} = \text{PPh}_3, \text{PEt}_2\text{Ph}, \text{PEt}_3,$ and $\text{P}(n\text{-butyl})_3$, and their ^1H NMR parameters have been determined.

Introduction

The activation of molecular hydrogen (dihydrogen) by transition metal complexes has been intensely investigated ever since the 1960s, when Wilkinson and co-workers discovered the first successful homogeneous hydrogenation catalyst $\text{RhCl}(\text{PPh}_3)_3$.^{1,2} Herewith terminal alkenes and alkynes can be readily hydrogenated at 25 °C at a hydrogen pressure of 1 bar.

The mechanism and kinetics thereof have been extensively studied, and some intermediate dihydrides such as $\text{Rh}(\text{H})_2\text{Cl}(\text{PPh}_3)_3$ and $\text{Rh}_2(\text{H})_2\text{Cl}_2(\text{PPh}_3)_4$ have been previously observed and characterized using NMR spectroscopy.^{3,4} The data available in the literature, however, are typically restricted to PPh_3 as the phosphine ligands, since in general the spectroscopic observation of such dihydride species is rather difficult. Due to their intermediate character, they have a short lifetime; hence they typically occur in rather low concentrations only. In this paper, we report the NMR data of some additional dihydrides of various mono- and binuclear Rh complexes containing different phosphine ligands, which have been detected in situ using parahydrogen-induced polarization (PHIP).⁵

Parahydrogen-Induced Polarization (PHIP)

Parahydrogen and orthohydrogen are the two nuclear spin isomers of dihydrogen, representing its nuclear singlet and triplet state, respectively. Parahydrogen, the singlet spin state, is magnetically inactive and hence invisible in the NMR spectrum. Therefore, any observed ^1H NMR resonance of dihydrogen is exclusively due to orthohydrogen. PHIP is based on the

PASADENA⁶ (parahydrogen and synthesis allow dramatically enhanced nuclear alignment) effect and originates from the breakdown of the initially high symmetry of parahydrogen as the consequence of a chemical reaction, which transfers the two formerly equivalent protons into either chemically or magnetically inequivalent positions. This transformation of the two hydrogen atoms has to occur pairwise during the hydrogenation. This means, that the initial A_2 spin system of parahydrogen becomes converted into an AB or AX spin system in the hydrogenation products. Thereby only those energy levels become selectively populated, which have some degree of singlet character. The details thereof depend on the boundary conditions, under which the hydrogenations are carried out, i.e., whether the reactions occur exclusively within the high magnetic field of the NMR spectrometer, as is the case here, or initially in the Earth's low magnetic field, upon which the samples are quickly transferred into the NMR spectrometer for immediate analysis. Either way, the ^1H PHIP NMR spectra of the parahydrogen-derived molecules show emission and absorption signals that are enhanced proportional to the reciprocal Boltzmann factor (typically by a few orders of magnitude) governing conventional NMR spectra recorded at the same magnetic field strength and temperature. As pointed out above, the occurrence of this phenomenon requires, however, that the transfer of the two parahydrogen atoms occurs in a pairwise manner, whereby the transferred protons experience some sort of coupling to each other at any time.

The considerable signal enhancement associated with PHIP allows detection of reaction intermediates and products at lower concentrations than is otherwise feasible using conventional NMR spectroscopy. Therefore, this method has been established as a versatile tool to investigate the structure of many hydrogen-containing transition metal complexes (typically dihydrides) and products of homogeneous hydrogenations.⁷

(1) Young, J. F.; Osborn, J. A.; Jardine, F. H.; Wilkinson, G. *J. Chem. Soc., Chem. Commun.* **1965**, 131–132.

(2) Osborn, J. A.; Jardine, F. H.; Young, J. F.; Wilkinson, G. *J. Chem. Soc. A* **1966**, 1711–1732.

(3) Duckett, S. B.; Newell, C. L.; Eisenberg, R. *J. Am. Chem. Soc.* **1994**, *116*, 10548–10556.

(4) Tolman, C. A.; Meakin, P. Z.; Lindner, D. L.; Jesson, J. P. *J. Am. Chem. Soc.* **1974**, *96*, 2762–2774.

(5) Natterer, J.; Bargon, J. *Prog. Nucl. Magn. Reson. Spectrosc.* **1997**, *31*, 293–315.

(6) Bowers, C. R.; Weitekamp, D. P. *J. Am. Chem. Soc.* **1987**, *109*, 5541–5542.

(7) Duckett, S. B.; Sleigh, C. J. *Prog. Nucl. Magn. Reson. Spectrosc.* **1999**, *34*, 71–92.

The Spin Density Matrix and the Product Operator Formalism

A theoretical interpretation of the PHIP phenomenon based on the product operator formalism⁸ allows us to forecast or interpret PHIP spectra. In this description, the spin density matrix of parahydrogen is represented by $\sigma_{\text{parahydrogen}} = I_1 I_2$. On transferring the parahydrogen molecule into an AX spin system during hydrogenation, its spin density matrix is propagated, governed by the Hamiltonian for weakly coupled systems. Averaging over the duration of the hydrogenation, the spin density matrix of the former two parahydrogen atoms in the resulting AX spin system of the hydrogenation product simplifies to $\sigma_{\text{PASADENA}} = I_{1z} I_{2z}$. The subscript *z* denotes the orientation in a Cartesian coordinate system, whereby *z* coincides with the direction of the external magnetic field, and the numbers mark the respective protons. By contrast, the spin density matrix of two hydrogen nuclei at thermal equilibrium, i.e., long after the reaction, is described by $\sigma_{\text{thermal}} = I_{1z} + I_{2z}$.

Application of a radio frequency pulse corresponding to the flip angle β and the phase γ to the initial magnetization $\sigma_{\text{PASADENA}} = I_{1z} I_{2z}$ generates three operator terms according to

$$I_{1z} I_{2z} \xrightarrow{\beta I_y} \cos^2 \beta I_{1z} I_{2z} + \cos \beta \sin \beta (I_{1z} I_{2x} + I_{1x} I_{2z}) + \sin^2 \beta I_{1x} I_{2x}$$

The first and the last term thereof represent zero and double quantum coherences, respectively, which cannot be detected under these conditions. However, the term in the middle corresponds to an observable single quantum coherence, which is maximized if the flip angle β equals $\pi/4$. Therefore, when recording PHIP spectra, β is set to half the conventional value used in ordinary NMR spectroscopy, where $\pi/2$ represents the optimal value.

This fact can be taken advantage of in order to eliminate interfering resonances stemming from unpolarized systems, i.e., from molecules which do not participate in the hydrogenation sequence. This includes the resonances stemming from the solvent, from unpolarized starting material, or from previously formed product molecules that have since reached thermal equilibrium. For this purpose, individual scans are accumulated, whereby the flip angles are alternated between $-\pi/4$ and $3\pi/4$, consecutively. As a consequence of this change of the flip angle by 180° between two consecutive pulses, the amplitudes of regular, i.e., of "thermal", NMR resonances alternate in signs, whereas the signs of the PHIP signals remain the same, irrespectively. Accordingly, upon accumulating the corresponding signals, the "unpolarized" resonances are suppressed and eliminated, whereas the "polarized" PHIP resonances add up and become accumulated to yield a better signal-to-noise ratio.

The single quantum coherence $I_{1z} I_{2x} + I_{1x} I_{2z}$ develops under the Hamiltonian for weakly coupled systems into the term $\sin(\pi J_{12} t)(I_{1y} + I_{2y})$. The sine modulation of the term $(I_{1y} + I_{2y})$, corresponding to the coupling between the transferred parahydrogen protons, is responsible for the observed antiphase splitting in the resonances of the PHIP spectra. By contrast, the regular "thermal" resonances of species, which are chemically uninvolved in the hydrogenation reactions, experience a cosine modulation governed by their respective couplings, resulting in in-phase splittings of the resonances in the PHIP NMR spectra. Likewise, couplings to protons which do not stem

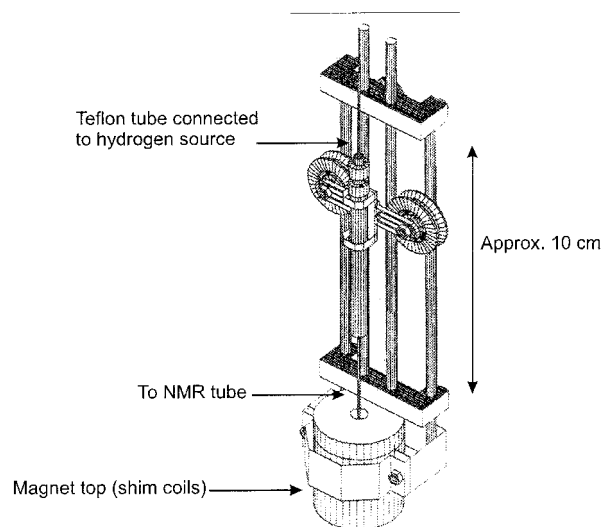


Figure 1. The apparatus used to carry out the hydrogenation inside of the NMR magnet. The device is installed on top of the magnet. Before the hydrogenation starts, the sled can be lowered by about 10 cm by means of the pulleys. Thereby a glass capillary connected to the parahydrogen source by means of a Teflon tube can be lowered into the NMR probe actuated by an electromagnet, which is electrically controlled by the computer of the NMR spectrometer.

from parahydrogen cause in-phase splittings in the PHIP resonances, just as is the case in regular ("thermal") NMR spectra.

In Situ PHIP NMR Spectroscopy of Homogeneous Hydrogenations

This paper describes the use of PHIP to detect some new dihydride products at low concentrations which can otherwise not be seen using conventional NMR methods. For this purpose, the hydrogenation with parahydrogen is carried out in situ using the apparatus in Figure 1, which allows us to monitor the reaction and thereby determine its kinetic constants.

Results and Discussion

Reactions of $[\text{RhCl}(\text{NBD})_2]$ with Parahydrogen in the Presence of Tertiary Phosphines. The binuclear precursor (di- μ -chlorobis[η^4 -2,5-norbornadiene]rhodium(I) = $[(\text{Rh}(\text{NBD})\text{Cl})_2]$) is well suited for the in situ preparation of a variety of homogeneous hydrogenation catalysts, if tertiary phosphines (here PMe_3 , PMe_2Ph , PMePh_2 , PEt_3 , PEt_2Ph , PEtPh_2 , or $\text{P}(n\text{-butyl})_3$) are added to the solution of this precursor. Upon the addition of dihydrogen to these mixtures, NBD is hydrogenated off, and the mononuclear dihydride species $\text{Rh}(\text{H})_2\text{ClL}_3$ is generated, most likely via the complex RhClL_3 as an intermediate. This dihydride complex plays a key role as an intermediate in any subsequent catalytic hydrogenation.

As a characteristic example, Figure 2a shows the results obtained upon the addition of parahydrogen to a solution of 10 mg $[\text{Rh}(\text{NBD})\text{Cl}]_2$ and 19 μL PMePh_2 in acetone- d_6 (Rh: P = 1:3). The strong polarized resonances of the dihydride protons of the complex $\text{Rh}(\text{H})_2\text{Cl}(\text{PMePh}_2)_3$ are observed in the ^1H NMR spectrum, whereby the hydride trans to a PMePh_2 ligand occurs at $\delta_{\text{H}} = -9.4$ ppm, whereas the hydride trans to the chloride has a higher chemical shift and appears at $\delta_{\text{H}} = -17.6$ ppm. The latter is characteristic for hydride protons in the trans position to such an electronegative ligand. The hydride resonance at lower field shows a large coupling to one trans phosphorus ($J_{\text{HP}(\text{trans})} = 178.6$ Hz), an additional coupling to two equivalent cis phosphorus nuclei ($J_{\text{HP}(\text{cis})} = 14.1$ Hz), a

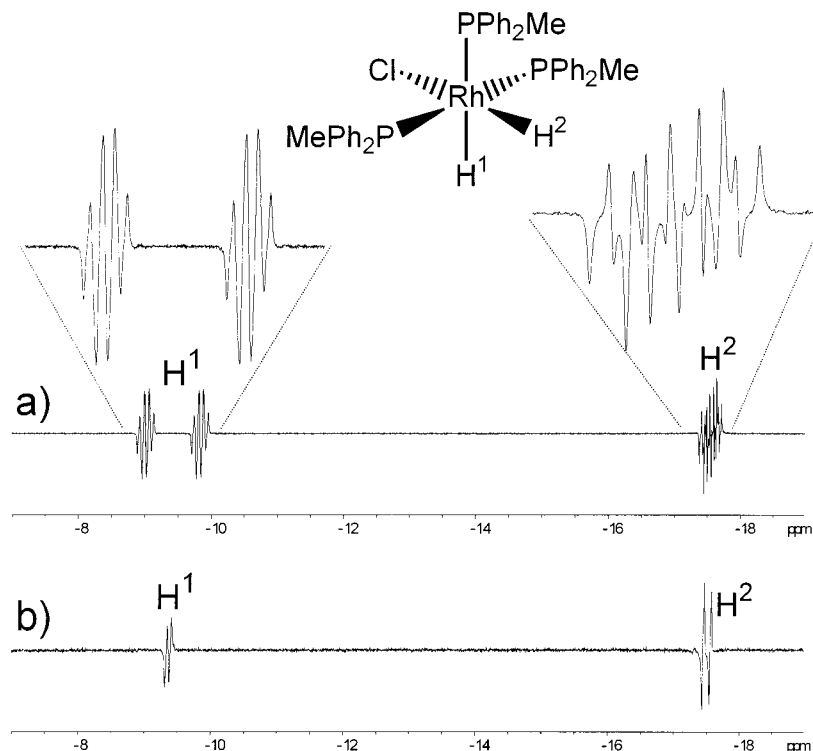


Figure 2. (a) The hydride region of the ^1H NMR spectra obtained using a sample of 10 mg of $[\text{Rh}(\text{NBD})\text{Cl}]_2$ and 19 μL of PMePh_2 in acetone- d_6 (Rh:P = 1:3) after the in situ addition of parahydrogen at 315 K. The spectrum shows the hydride resonances of the complex $\text{Rh}(\text{H})_2\text{Cl}(\text{PMePh}_2)_3$, **3**, which have been recorded with eight scans. The hydrides have been enlarged above the original spectra. (b) $^1\text{H}\{^{31}\text{P}\}$ NMR spectra of the hydride region with ^{31}P broadband decoupling.

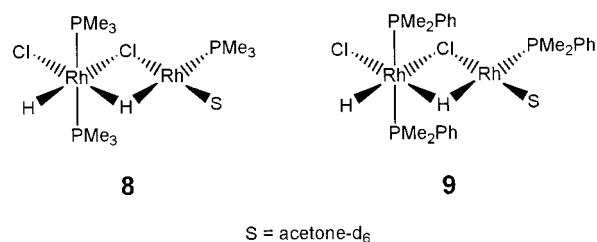
coupling to the central rhodium ($J_{\text{HRh}} = 13$ Hz), and a coupling to the upfield hydride proton ($J_{\text{HH}_-} = -7.7$ Hz). The coupling between the two former parahydrogen protons causes the antiphase character of this resonance, exhibiting emission and absorption maxima, accordingly. The second hydride resonance at higher field is a complex multiplet with couplings to rhodium ($J_{\text{HRh}} = 22$ Hz), one equatorial and two axial phosphorus nuclei ($J_{\text{HP(ax)}} = 16.5$ Hz, $J_{\text{HP(eq)}} = 11$ Hz), and the lower field hydride proton ($J_{\text{HH}_-} = -7.7$ Hz). These data have been tested by simulating the resulting multiplet and polarization pattern using the computer program PHIP++, upon which very good agreement has been obtained.⁹ If the ^1H NMR spectrum is recorded with complete ^{31}P decoupling, both hydride resonances at -9.4 and -17.6 ppm collapse into a doublet of antiphase doublets with the remaining 13 and 22 Hz coupling corresponding to J_{HRh} and J_{HRh_-} , respectively (Figure 2b). Analogous complexes with other phosphine ligands have also been observed (Table 1).

If the temperature is elevated, the intensities of the polarized hydride resonances increase significantly. The spectrum displayed in Figure 2a has been recorded at 315 K. Experiments in acetone- d_6 can be carried out up to about 330 K, since above this value, boiling and associated evaporation of the solvent becomes so significant that this deteriorates the resolution of the spectra badly.

By contrast, the resolution of the corresponding hydride resonances deteriorates with increasing temperature. For better resolution, therefore, a lower temperature is advantageous, since the rate of phosphine dissociation slows down with decreasing temperature, upon which the resonances sharpen.

The rate of the observed exchange reaction of the phosphine ligands in the dihydrides increases in the above-listed series of

Scheme 1



phosphines from PMe_3 to $\text{P}(n\text{-butyl})_3$ (Table 1), which in turn correlates with the activity of the corresponding complexes as hydrogenation catalysts.

Furthermore, the intensities of the polarized hydride resonances increase with temperature. Since these intensities correlate with the rate of oxidative addition of parahydrogen to the corresponding rhodium complexes and with the subsequent decay of the so-formed dihydrides, both the rates of their formation as well as the rates of their decay seem to increase with temperature.

Formation of the Binuclear Complexes $(\text{H})(\text{Cl})\text{Rh}(\text{PMe}_3)_2(\mu\text{-Cl})(\mu\text{-H})\text{Rh}(\text{PMe}_3)_2$ and $(\text{H})(\text{Cl})\text{Rh}(\text{PMe}_2\text{Ph})_2(\mu\text{-Cl})(\mu\text{-H})\text{Rh}(\text{PMe}_2\text{Ph})_2$. Upon addition of parahydrogen to a solution of $[\text{RhCl}(\text{NBD})]_2$ and PMe_3 (ratio of Rh: P = 1:3) in acetone- d_6 at 315 K, intense polarization signals of the dihydride complex $\text{Rh}(\text{H})_2\text{Cl}(\text{PMe}_3)_3$ (**1**) can be observed along with strongly polarized resonances in the aliphatic region due to hydrogenation of the NBD ligand. This complex **1** has been described earlier by other authors.¹⁰ In later stages of the reaction, however, two new resonances emerge at -18.2 and -20.2 ppm, respectively (Figure 3a), which can be assigned to the hydride protons of the complex **8** in Scheme 1. These signals too have antiphase character due to the coupling between the two parahydrogen protons ($J_{\text{HH}'} = -4.2$ Hz). Thereby the hydride resonance at

(9) Greve, T. PhD Thesis, Physics, University of Bonn 1996.

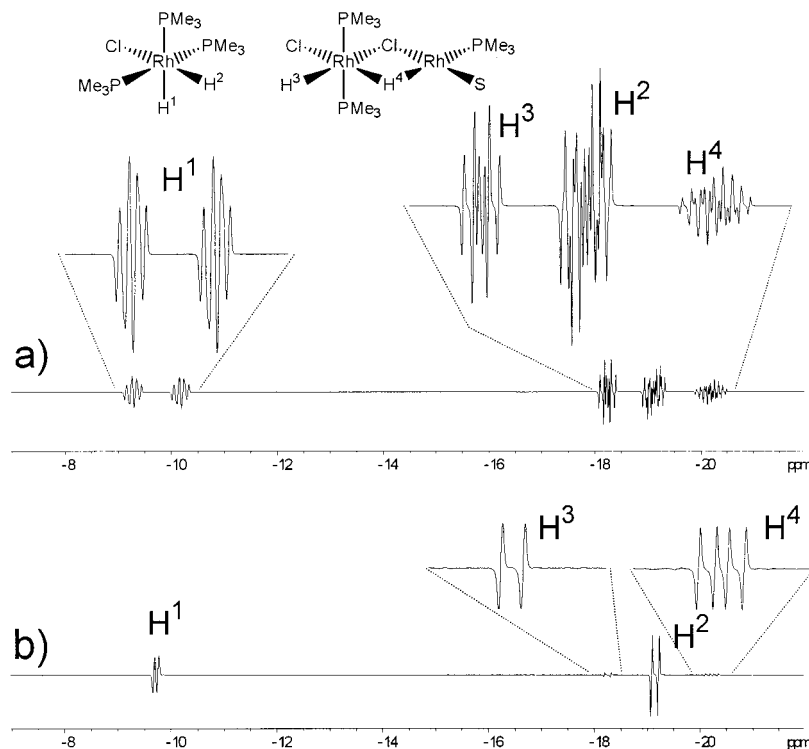


Figure 3. (a) The hydride region of the ^1H NMR spectra obtained using a sample of 10 mg of $[\text{Rh}(\text{NBD})\text{Cl}]_2$ and 13.2 μL of PMe_3 in acetone- d_6 ($\text{Rh}:\text{P} = 1:2$) after the in situ addition of parahydrogen at 320 K. The spectrum shows the hydride resonances of the complex $\text{Rh}(\text{H})_2\text{Cl}(\text{PMe}_3)_3$, **1**, and $(\text{H})(\text{Cl})\text{Rh}(\text{PMe}_3)_2(\mu\text{-Cl})(\mu\text{-H})\text{Rh}(\text{PMe}_3)_3$, **8**. (b) $^1\text{H}\{^{31}\text{P}\}$ NMR spectra of the hydride region with ^{31}P broadband decoupling ($\text{S} = \text{acetone-}d_6$).

Table 1. ^1H NMR Data of the Reported Hydrides

no.	complex	^1H chemical shifts δ (ppm) in acetone- d_6 and coupling constants J (Hz)
1	$\text{Rh}(\text{H})_2\text{Cl}(\text{PMe}_3)_3$	-9.7 ($^1J_{\text{HRh}} = 15$, $^2J_{\text{HP}(\text{trans})} = 178.6$, $^2J_{\text{HP}(\text{cis})} = 20$, $^2J_{\text{HH}} = -7.5$) -19.0 ($^1J_{\text{HRh}} = 27$, $^2J_{\text{HP}(\text{ax.})} = 19$, $^2J_{\text{HP}(\text{eq.})} = 13$, $^2J_{\text{HH}} = -7.5$)
2	$\text{Rh}(\text{H})_2\text{Cl}(\text{PMe}_2\text{Ph})_3$	-9.6 ($^1J_{\text{HRh}} = 18$, $^2J_{\text{HP}(\text{trans})} = 172.5$, $^2J_{\text{HP}(\text{cis})} = 18$, $^2J_{\text{HH}} = -7.2$) -18.2 ($^1J_{\text{HRh}} = 24.7$, $^2J_{\text{HP}(\text{ax.})} = 16.5$, $^2J_{\text{HP}(\text{eq.})} = 11$, $^2J_{\text{HH}} = -7.2$)
3	$\text{Rh}(\text{H})_2\text{Cl}(\text{PMePh}_2)_3$	-9.4 ($^1J_{\text{HRh}} = 13$, $^2J_{\text{HP}(\text{trans})} = 164$, $^2J_{\text{HP}(\text{cis})} = 14.1$, $^2J_{\text{HH}} = -7.7$) -17.6 ($^1J_{\text{HRh}} = 22$, $^2J_{\text{HP}(\text{ax.})} = 15$, $^2J_{\text{HP}(\text{eq.})} = 10$, $^2J_{\text{HH}} = -7.7$)
4	$\text{Rh}(\text{H})_2\text{Cl}(\text{PEt}_3)_3$	-10.7 ($^1J_{\text{HRh}} = 14.7$, $^2J_{\text{HP}(\text{trans})} = 161.7$, $^2J_{\text{HP}(\text{cis})} = 16$, $^2J_{\text{HH}} = -7.9$) -19.8 ($^1J_{\text{HRh}} = 24.1$, $^2J_{\text{HP}(\text{ax.})} = 16$, $^2J_{\text{HP}(\text{eq.})} = 13$, $^2J_{\text{HH}} = -7.9$)
5	$\text{Rh}(\text{H})_2\text{Cl}(\text{PEt}_2\text{Ph})_3$	-10.1 ($^1J_{\text{HRh}} = 15.4$, $^2J_{\text{HP}(\text{trans})} = 162$, $^2J_{\text{HP}(\text{cis})} = 16.3$, $^2J_{\text{HH}} = -7.3$) -19.3 ($^1J_{\text{HRh}} = 24.6$, $^2J_{\text{HP}(\text{ax.})} = 17$, $^2J_{\text{HP}(\text{eq.})} = 15.1$, $^2J_{\text{HH}} = -7.3$)
6	$\text{Rh}(\text{H})_2\text{Cl}(\text{PEtPh}_2)_3$	-9.9 ($^1J_{\text{HRh}} = 12.5$, $^2J_{\text{HP}(\text{trans})} = 155$, $^2J_{\text{HP}(\text{cis})} = 13.3$, $^2J_{\text{HH}} = -7.9$) -18.3 ($^1J_{\text{HRh}} = 20$, $^2J_{\text{HP}(\text{ax.})} = 12.5$, $^2J_{\text{HP}(\text{eq.})} = 13.5$, $^2J_{\text{HH}} = -7.9$)
7	$\text{Rh}(\text{H})_2\text{Cl}(\text{P}(n\text{-butyl})_3)_3$	-10.7 ($^1J_{\text{HRh}} = 13.5$, $^2J_{\text{HP}(\text{trans})} = 163$, $^2J_{\text{HP}(\text{cis})} = 16.7$, $^2J_{\text{HH}} = -7.8$) -19.8 ($^1J_{\text{HRh}} = 23$, $^2J_{\text{HP}(\text{ax.})} = 15.8$, $^2J_{\text{HP}(\text{eq.})} = 13.1$, $^2J_{\text{HH}} = -7.8$)
8	$(\text{H})(\text{Cl})\text{Rh}(\text{PMe}_3)_2(\mu\text{-Cl})(\mu\text{-H})\text{Rh}(\text{PMe}_3)_3$	-18.2 ($^1J_{\text{HRh}} = 25$, $^2J_{\text{HP}(\text{cis})} = 17.3$, $^2J_{\text{HH}} = -4.2$) -20.2 ($^1J_{\text{HRh}} = 30.3$, 20 , $^2J_{\text{HP}(\text{trans})} = 29$, $^2J_{\text{HP}(\text{cis})} = 14.6$, $^2J_{\text{HH}} = -4.2$)
9	$(\text{H})(\text{Cl})\text{Rh}(\text{PMe}_2\text{Ph})_2(\mu\text{-Cl})(\mu\text{-H})\text{Rh}(\text{PMe}_2\text{Ph})_3$	-17.3 ($^1J_{\text{HRh}} = 23$, $^2J_{\text{HP}(\text{cis})} = 15.4$, $^2J_{\text{HH}} = -4.2$) -20.0 ($^1J_{\text{HRh}} = 30$, 21.4 , $^2J_{\text{HP}(\text{trans})} = 29$, $^2J_{\text{HP}(\text{cis})} = 15.5$, $^2J_{\text{HH}} = -4.2$)
10	$\text{Rh}(\text{H})_2(\text{CF}_3\text{COO})(\text{PPh}_3)_3$	-8.9 ($^1J_{\text{HRh}} = 6$, $^2J_{\text{HP}(\text{trans})} = 161$, $^2J_{\text{HP}(\text{cis})} = 12$, $^2J_{\text{HH}} = -9.5$) -19.1 ($^1J_{\text{HRh}} = 18$, $^2J_{\text{HP}(\text{ax.})} = 17$, $^2J_{\text{HP}(\text{eq.})} = 17$, $^2J_{\text{HH}} = -9.5$)
11	$\text{Rh}(\text{H})_2(\text{CF}_3\text{COO})(\text{PEt}_3)_3$	-10.1 ($^1J_{\text{HRh}} = 14.8$, $^2J_{\text{HP}(\text{trans})} = 160$, $^2J_{\text{HP}(\text{cis})} = 16$, $^2J_{\text{HH}} = -8.7$) -22.5 ($^1J_{\text{HRh}} = 13$, $^2J_{\text{HP}(\text{ax.})} = 17$, $^2J_{\text{HP}(\text{eq.})} = 17$, $^2J_{\text{HH}} = -8.7$)
12	$\text{Rh}(\text{H})_2(\text{CF}_3\text{COO})(\text{PEt}_2\text{Ph})_3$	-9.5 ($^1J_{\text{HRh}} = 15.5$, $^2J_{\text{HP}(\text{trans})} = 161$, $^2J_{\text{HP}(\text{cis})} = 16.8$, $^2J_{\text{HH}} = -8.6$) -21.9 ($^1J_{\text{HRh}} = 26.8$, $^2J_{\text{HP}(\text{ax.})} = 16.7$, $^2J_{\text{HP}(\text{eq.})} = 16.7$, $^2J_{\text{HH}} = -8.6$)
13	$\text{Rh}(\text{H})_2(\text{CF}_3\text{COO})(\text{P}(n\text{-butyl})_3)_3$	-9.5 ($^1J_{\text{HRh}} = 15.5$, $^2J_{\text{HP}(\text{trans})} = 161.5$, $^2J_{\text{HP}(\text{cis})} = 16.7$, $^2J_{\text{HH}} = -7.1$) -21.9 ($^1J_{\text{HRh}} = 28.8$, $^2J_{\text{HP}(\text{ax.})} = 17.5$, $^2J_{\text{HP}(\text{eq.})} = 17.5$, $^2J_{\text{HH}} = -7.1$)

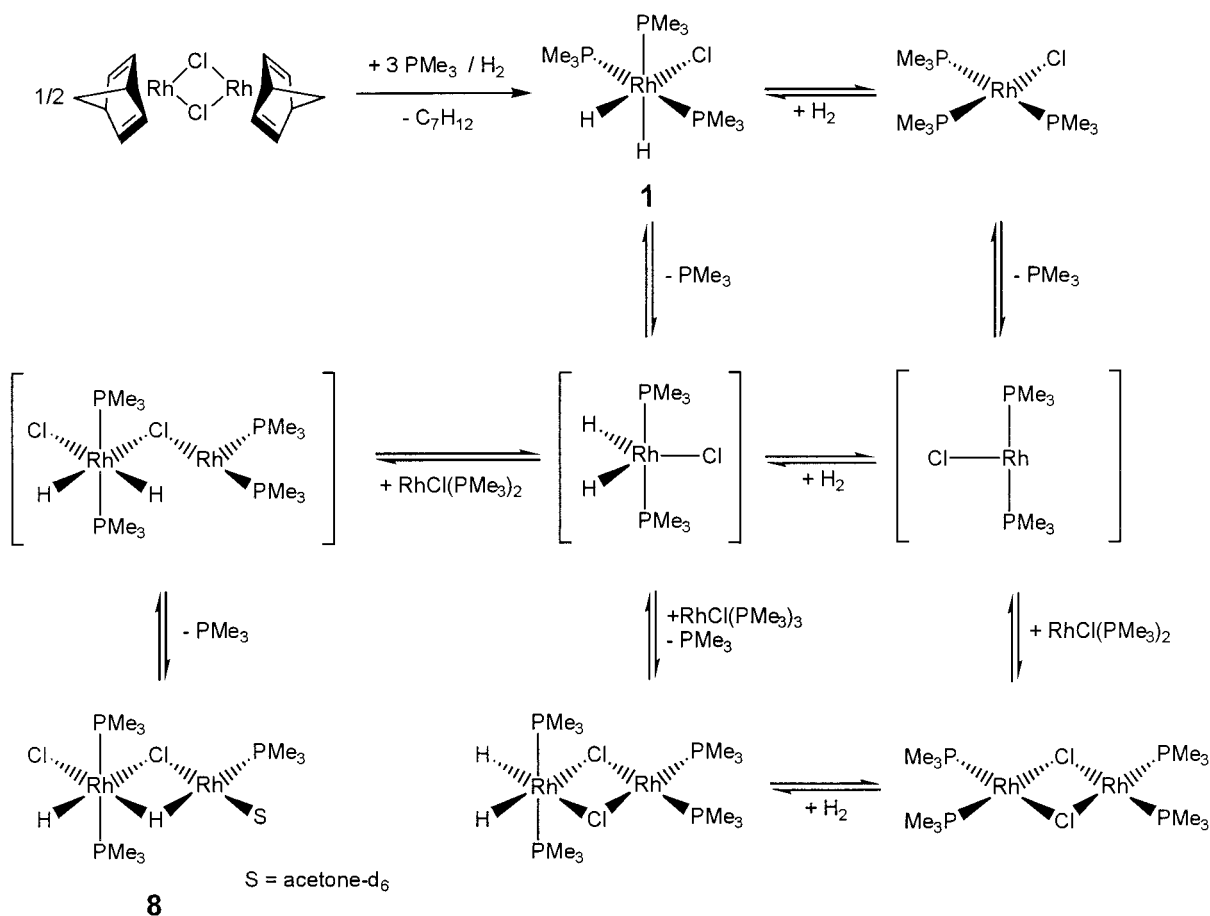
-18.2 ppm exhibits a coupling to rhodium ($J_{\text{HRh}} = 25$ Hz) and the cis phosphorus ($J_{\text{HP}(\text{cis})} = 17.3$ Hz), whereas the second hydride resonance consists of a complex multiplet with couplings to the two inequivalent rhodium atoms ($J_{\text{HRh}} = 30.3$ Hz and $J_{\text{Rh}^{\text{H}}} = 20$ Hz, respectively), the two cis phosphorus nuclei ($J_{\text{HP}(\text{cis})} = 14.6$ Hz), and the trans phosphorus ($J_{\text{HP}(\text{trans})} = 29$ Hz). This assignment is confirmed upon ^{31}P decoupling of the

hydride protons: In the $^1\text{H}\{^{31}\text{P}\}$ NMR spectrum shown in Figure 3b, the signal at -18.2 ppm has collapsed into a doublet of antiphase doublets with the 25 Hz coupling corresponding to J_{HRh} , while the second hydride resonance has simplified to a doublet of doublet of antiphase doublets, with couplings of 30.3 and 20 Hz corresponding to J_{HRh} and $J_{\text{HRh}'}$, respectively.

Complexes of the type $(\text{H})(\text{Cl})\text{Rh}(\text{PMe}_3)_2(\mu\text{-Cl})(\mu\text{-H})\text{Rh}(\text{CO})(\text{PMe}_3)$ and $(\text{H})(\text{Cl})\text{Rh}(\text{PMe}_3)_2(\mu\text{-I})(\mu\text{-H})\text{Rh}(\text{CO})(\text{PMe}_3)$, the NMR data of which correspond to our results, have been

(10) Duckett, S. B.; Eisenberg, R.; Goldman, A. S. *J. Chem. Soc., Chem. Commun.* **1993**, 1185–1187.

Scheme 2



detected using PHIP NMR spectroscopy.^{11,12} In these studies the phosphine ligand at the rhodium(I) center is supposed to be trans to the μ -hydride with a phosphorus coupling of $J_{\text{HP}(\text{trans})} = 30$ and 32 Hz, respectively. Therefore, the structure in Scheme 1 is assigned to complex **8**. Since in our experiments no carbon monoxide is present, the fourth position of the Rh(I) center could be occupied by the solvent (acetone- d_6). The polarized resonances in the aliphatic region due to hydrogenation of NBD and its hydrogenation product NBE only occur at the beginning of the reaction. At the same time complex **1** can be observed. When the hydrogenation of NBD and NBE is completed only complex **1** is present. The ^1H NMR spectrum shows only resonances of norbornane. With the proceeding hydrogenation complex **8** emerges. Therefore, we have ruled out that the fourth ligand at the rhodium(I) center is occupied by NBE. In the study of Wilkinson's catalyst, Duckett and Eisenberg have reported binuclear complexes containing an olefin at the rhodium(I) center.³

During the hydrogenation the solution is turning dark brown, and black rhodium metal is precipitating. Even though complex **1** gradually disappears and complex **8** emerges during the hydrogenation until eventually only the polarization signals of **8** are visible, adding new PMe_3 to the solution reverses the process, causing the resonances of complex **8** to get weaker and those of complex **1** to reappear again. However, using an excess of PMe_3 from the beginning of the experiment on leads to the appearance of polarization signals due to the complex

$(\text{H})_2\text{Rh}(\text{PMe}_3)_4^+$, which has been described earlier by Schrock and Osborn.¹³

Analogously, complex **9**, with PMe_2Ph as the phosphine ligand instead of PMe_3 , can be obtained and its ^1H PHIP NMR spectrum can be observed under the same conditions. The formation of this binuclear rhodium dihydride can be explained according to Scheme 2.

The five-coordinate species $\text{Rh}(\text{H})_2\text{Cl}(\text{PMe}_3)_2$ is formed after phosphine dissociation from **1** and H_2 addition to the 14-electron complex $\text{RhCl}(\text{PMe}_3)_2$. The resulting 16-electron species coordinates an alkene under catalytic conditions to form an addition complex which functions as a key intermediate in the catalytic cycle. Subsequently, this coordinatively unsaturated dihydride completes its coordination shell via complexation with the chloride ligand of $\text{RhCl}(\text{PMe}_3)_2$, which is followed by displacement of a phosphine to form the Rh(III)/Rh(I) binuclear complex **8**. The identity of the 14-electron species $\text{RhCl}(\text{PMe}_3)_2$ has been confirmed for the phosphine ligands PMe_3 , $\text{P}(\text{tolyl})_3$, and PPh_3 before by other authors.^{14,15} In particular, the reaction of Wilkinson's catalyst $\text{RhCl}(\text{PPh}_3)_3$ with H_2 leads at elevated temperature to the formation of the Rh(III)/Rh(I) binuclear complex $(\text{H})_2\text{Rh}(\text{PPh}_3)_2(\mu\text{-Cl})_2\text{Rh}(\text{PPh}_3)_2$, which was first identified by Tolman et al.⁴ This complex is in equilibrium with $\text{Rh}(\text{PPh}_3)_2(\mu\text{-Cl})_2\text{Rh}(\text{PPh}_3)_2$, which is a dimerization product of $\text{RhCl}(\text{PPh}_3)_2$.

A related complex can also be observed with PMe_3 as the phosphine, if the hydrogenation is carried out at a low rhodium/

(11) Duckett, S. B.; Eisenberg, R. *J. Am. Chem. Soc.* **1993**, *115*, 5292–5293.

(12) Morran, P. D.; Colebrooke, S. A.; Duckett, S. B.; Lohman, J. A. B.; Eisenberg, R. *J. Chem. Soc., Dalton Trans.* **1998**, 3363–3365.

(13) Schrock, R. R.; Osborn, J. A. *J. Am. Chem. Soc.* **1971**, *93*, 2397–2406.

(14) Wink, D.; Ford, P. C. *J. Am. Chem. Soc.* **1985**, *107*, 1794–1796.

(15) Spillet, C. T.; Ford, P. C. *J. Am. Chem. Soc.* **1989**, *111*, 1932–1933.

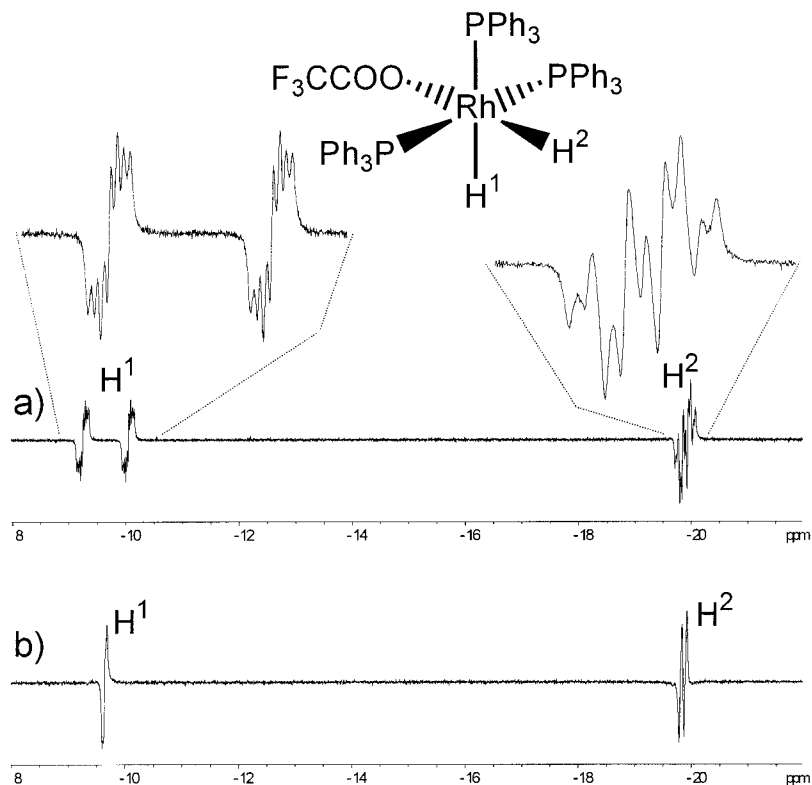
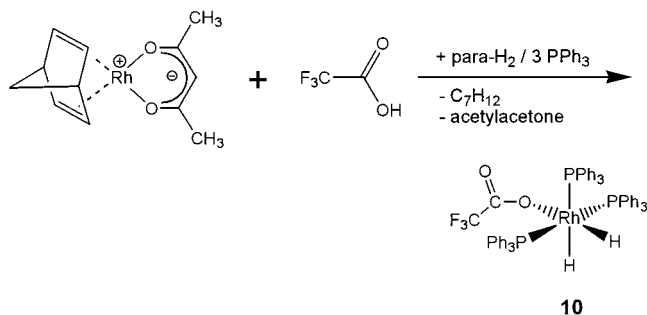


Figure 4. (a) The hydride region of the ^1H NMR spectra obtained using a sample of 10 mg of $\text{Rh}(\text{NBD})(\text{acac})$, 13.5 mg of PPh_3 , and 1 μL of CF_3COOH in $\text{acetone-}d_6$ ($\text{Rh}:\text{P} = 1:3$) after the in situ addition of parahydrogen at 300 K. The spectrum shows the hydride resonances of the complex $\text{Rh}(\text{H})_2(\text{CF}_3\text{COO})(\text{PPh}_3)_3$, **10**, which have been recorded with eight scans. The hydrides have been enlarged above the original spectra. (b) $^1\text{H}\{^{31}\text{P}\}$ NMR spectra of the hydride region with ^{31}P broadband decoupling.

Scheme 3



phosphine ratio ($\text{Rh}:\text{P} = 1:1$) at 325 K. However, this complex is characterized by an unpolarized resonance at -19.8 ppm, possibly of a monohydride, which consists of a doublet of triplets with $J_{\text{HRh}} = 24.7$ Hz and $J_{\text{HP}} = 19.4$ Hz, respectively.

Generation of $\text{Rh}(\text{NBD})(\text{PPh}_3)_3(\text{CF}_3\text{COO})$ and Its Dihydride. The dihydrido rhodium(III) complexes as described above so far have chloride as the electronegative ligand. The latter can readily be replaced by trifluoroacetate. For this purpose, a solution of $\text{Rh}(\text{NBD})(\text{acac})$ ($\text{acac} = \text{acetylacetonate}$) and PPh_3 in $\text{acetone-}d_6$ is treated with CF_3COOH . Upon that, the initial acetylacetonate ligand is displaced from the rhodium center after protonation (Scheme 3).

Adding parahydrogen to this three-component solution leads to the occurrence of strongly polarized resonances of norbornene and norbornane in the aliphatic region of the ^1H PHIP NMR spectrum, due to hydrogenation of the NBD ligand. In addition, two hydride resonances of the complex $\text{Rh}(\text{H})_2(\text{CF}_3\text{COO})(\text{PPh}_3)_3$ (**10**) emerge at -8.9 and -19.1 ppm, respectively (Figure 4a). The resonance of the hydride proton at lower field exhibits a trans phosphorus coupling ($J_{\text{HP}}(\text{trans}) = 161$ Hz) with an

additional coupling of 12 Hz to the cis phosphorus, a 6 Hz coupling to rhodium, and an antiphase coupling due to the second hydrogen ($J_{\text{HH}'} = -9.5$), which causes the observed emission and absorption maxima. The second hydride proton, whose chemical shift at higher field is characteristic for hydrides in the trans position to a rather electronegative ligand (here trifluoroacetate), gives a complex multiplet with couplings to rhodium ($J_{\text{HRh}} = 18$ Hz), two equivalent cis phosphine ligands ($J_{\text{HP}} = 17$ Hz), and the other hydride proton at lower field ($J_{\text{HH}'} = -9.5$ Hz). If the ^1H PHIP NMR spectrum is recorded with complete ^{31}P decoupling, both hydride resonances at -8.9 and -19.1 ppm collapse into a doublet of antiphase doublets with the remaining 6 and 18 Hz coupling corresponding to J_{HRh} and $J_{\text{HRh}'}$, respectively (Figure 4b).

Additional dihydride complexes can be observed using PEt_3 , PET_2Ph , or $\text{P}(n\text{-butyl})_3$ as the phosphine ligands. In the case of the ligands PET_2Ph or $\text{P}(n\text{-butyl})_3$, the resonances of the dihydrides are broadened due to the fast exchange of these phosphine ligands, which blurs the resonances of the hydride protons. Upon cooling the sample, the rate of this exchange process can be slowed, resulting in improved resolution, as is evident in Figure 1.

As a characteristic example, a solution of $\text{Rh}(\text{NBD})(\text{acac})$ and PET_2Ph in $\text{acetone-}d_6$ has been treated with CF_3COOH . Adding parahydrogen generates the complex $\text{Rh}(\text{H})_2(\text{CF}_3\text{COO})(\text{PET}_2\text{Ph})_3$ (**12**). Hydrogenation at decreasing temperatures (290, 273, and 263 K, respectively) results in a line narrowing of the hydride resonances. At 263 K the multiplets are well-resolved. However, upon decreasing the temperature, the intensities of the hydride resonances get weaker, because the rate of parahydrogen addition slows down, until below 253 K the rhodium dihydride, **12**, cannot be observed anymore.

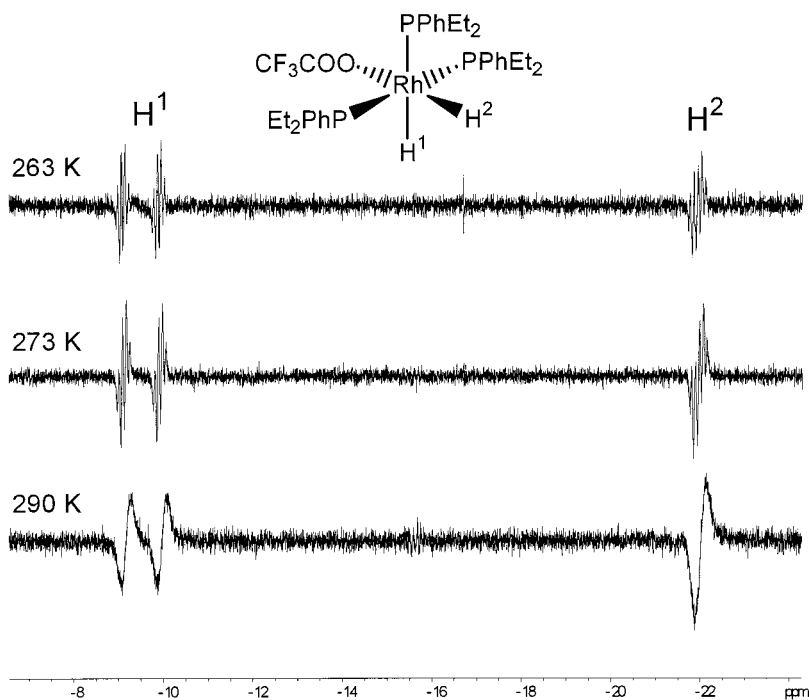


Figure 5. The hydride region of the ^1H NMR spectra obtained using a sample of 10 mg of $\text{Rh}(\text{NBD})(\text{acac})$, 8.5 mg of PEt_2Ph , and 1 μL of CF_3COOH in acetone- d_6 ($\text{Rh}:\text{PEt}_2\text{Ph} = 1:3$) after the in situ addition of parahydrogen at different temperatures. The spectrum shows the hydride resonances of the complex $\text{Rh}(\text{H})_2(\text{CF}_3\text{COO})(\text{PEt}_2\text{Ph})_3$, **12**, which have been recorded with eight scans.

Upon using either acetic acid or tetrafluoroboric acid, however, instead of trifluoroacetic acid, no analogous rhodium-containing dihydrides can be observed.

A few similar complexes containing rhodium have been described before by other authors.¹⁶

Experimental Section

The two complexes, i.e., $[\text{RhCl}(\text{NBD})]_2$ and $\text{Rh}(\text{NBD})(\text{acac})$, as well as trifluoroacetic acid and the phosphines PMe_3 , PMe_2Ph , PMePh_2 , PEt_3 , PEt_2Ph , PEtPh_2 , and $\text{P}(n\text{-butyl})_3$, have all been purchased from Aldrich and used as obtained. The solvent acetone- d_6 (Eurisotop) has been dried using standard methods and stored under argon prior to use. Chemical shift values are given in ppm using acetone- d_6 at 2.05 ppm as internal reference.

The spectra were recorded using either a Bruker AC 200 or a Bruker AMX 200 FT-NMR spectrometer, whereby the latter allowed ^{31}P decoupling. All spectra are the result of the accumulation of eight scans while alternating the flip angle between $-\pi/4$ and $+3\pi/4$, respectively, to suppress any thermal signals.

In Situ Hydrogenation Using Parahydrogen. Para-enriched hydrogen containing about 50% para- H_2 is prepared by passing H_2 through activated charcoal at 77 K at a pressure of 3 bar as described in the literature.⁵

The hydrogenation with parahydrogen is carried out in situ (Figure 1). For this purpose, a glass capillary connected to the parahydrogen source can be lowered into the NMR probe actuated by an electromagnet, i.e., by a solenoid, which is electrically controlled by the computer of the NMR spectrometer. In this fashion, parahydrogen can

be bubbled through the reaction mixture for a defined period of time followed by the detection pulse of the NMR experiment. In most cases, a hydrogenation time of 3 s has turned out to be sufficient. About 2 s after the hydrogen addition has stopped, the NMR detection can start. This procedure can be repeated to afford a subsequent accumulation of several scans, which yields a good signal-to-noise ratio of the PHIP resonances and allows us to suppress signals of components, which are uninvolved in the hydrogenation as outlined above. The spectrum in Figure 2 is the result of the accumulation of 16 scans, thereby alternating the flip angles between $-\pi/4$ and $+3\pi/4$, respectively, to suppress any thermal signals.

General Procedure for the in Situ Generation of the Complexes $\text{Rh}(\text{H})_2\text{CIL}_3$ (L = Phosphine). In a typical experiment, the rhodium complex $[\text{RhCl}(\text{NBD})]_2$ (10 mg) and the corresponding amount of phosphine ligand ($\text{Rh}:\text{P} = 1:3$) are placed into an NMR tube together with 700 μL of degassed acetone- d_6 . Parahydrogen is then bubbled in situ through the solution within the magnetic field of the spectrometer using the apparatus as outlined above.

General Procedure for the in Situ Generation of the Complexes $\text{Rh}(\text{H})_2(\text{CF}_3\text{COO})\text{L}_3$ (L = Phosphine). Likewise, the complex $\text{Rh}(\text{NBD})(\text{acac})$ (10 mg) together with trifluoroacetic (1 μL) acid and the corresponding amount of phosphine ligand ($\text{Rh}:\text{P} = 1:3$) is dissolved in 700 μL of acetone- d_6 and treated as described above.

Acknowledgment. We gratefully acknowledge the financial support obtained from the Volkswagen Foundation, the Deutsche Forschungsgemeinschaft (DFG), the German Federal Ministry for Science and Technology (BMBF), the Forschungsverband Nordrhein-Westfalen, and the Fonds der Chemischen Industrie, Frankfurt (Main), Germany.

(16) Esteruelas, M. A.; Lahuerta, O.; Modrego, J.; Nürnberg, O.; Oro, L. A.; Rodríguez, L.; Sola, E.; Werner H. *Organometallics* **1993**, *12*, 266–275.